

AiDAC: A Low-Cost In-Memory Computing Architecture with All-Analog Multi-Bit Compute and Interconnect

Zihao Xuan^{1,2}, Song Chen¹, Yi Kang^{1*}

¹ School of Microelectronics, University of Science and Technology of China, Hefei, China

² AI Chip Center for Emerging Smart Systems, The Hong Kong University of Science and Technology, Hong Kong, China

*Email: ykang@ustc.edu.cn

Abstract—Analog in-memory computing (AiMC) is an emerging technology that shows fantastic performance superiority for neural network acceleration. However, as the computational bit-width and scale increase, high-precision data conversion and long-distance data routing will result in unacceptable energy and latency overheads in the AiMC system. In this work, we focus on the potential of in-charge computing and in-time interconnection and show an innovative AiMC architecture, named AiDAC, with three key contributions: (1) AiDAC enhances multibit computing efficiency and reduces data conversion times by grouping capacitors technology; (2) AiDAC first adopts row drivers and column time accumulators to achieve large-scale AiMC arrays integration while minimizing the energy cost of data movements. (3) AiDAC is the first work to support large-scale all-analog multibit vector-matrix multiplication (VMM) operations. The evaluation shows that AiDAC maintains high-precision calculation (less than 0.79% total computing error) while also possessing excellent performance features, such as high parallelism (up to 26.2TOPS), low latency (<20ns/VMM), and high energy efficiency (123.8TOPS/W), for 8bits VMM with 1024 input channels.

Index Terms—Analog In-memory Computing, Neural Network Accelerating, Vector-Matrix Multiplication, Multibit Operation.

I. INTRODUCTION

In the ever-evolving landscape of artificial intelligence (AI), there is also a growing demand for innovative computing hardware solutions[1]. Among many emerging computing paradigms, one promising approach is in-memory computing (IMC)[2], a technology that eliminates the primary energy consumption overhead caused by data access and storage by fusing computing units into memory. Compared to traditional computing systems such as von Neumann’s, IMC systems no longer need to frequently distribute data between memory and processing units, and processing programs are executed directly in high-density memory arrays. It provides an excellent computing paradigm with extremely low power consumption, high energy efficiency, and high throughput in memory access and computation.

IMC circuits are divided into digital-type IMC (DiMC) and analog-type IMC (AiMC), while the former adopts massive digital multipliers and adders to implement parallel computations, and the latter is a creative technique that takes inspiration from the natural laws of physics to execute computations, such as Kirchhoff’s voltage and current law[3, 4]. Compared to DiMC, AiMC has a theoretical performance advantage. However, this

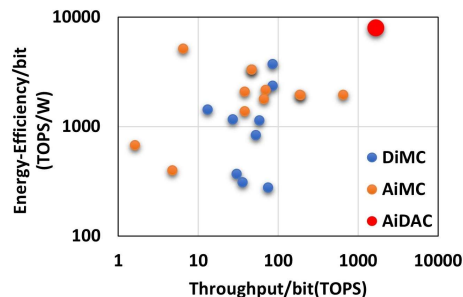


Fig. 1. Normalized throughput versus energy efficiency of recent IMCs.

advantage is still in the air so far (see Fig. 1), especially in high-precision and large-scale computing scenarios. Several key challenges hinder its practical implementation and widespread adoption: (1) The analog method has low computational accuracy due to signal margin and process variation and is limited to low bit width computational applications, such as binary and ternary DNNs (BNNs and TNNs); (2) existing analog computing mechanisms are not superior enough for multi-bit operations, and peripheral weighting circuits lead to additional cost of energy and time; (3) the overhead of high-precision analog-to-digital (AD) and digital-to-analog (DA) converters limits AiMC energy- and area-efficiency; (4) long-distance and intense movement of inputs and partial sums in buffers cause performance bottleneck for AiMC.

To address these challenges, this work notes the opportunities of high precision multibit compute in charge domain and local interconnect in time domain. The main contributions are as follows:

- We first propose an all-in-charge AiMC macro for energy-saving and high-precision (0.68% in-charge MAC error) multi-bit VMM by grouping capacitors.
- We presented a minimizing data movements strategy by integrating macros in analog-domain by low-cost row drivers and high signal margin column time accumulators (0.11% in-time summation error).
- We show a novel AiMC architecture, called AiDAC (Analog In-memory-computing for Data Arithmetic Computing), that first realizes all-analog multibit computing with excellent energy efficiency (up to 123.8 TOPS/W) and throughput (up to 26.2 TOPS).
- We compare our design with 8 state-of-the-art (SOTA) cases and show that AiDAC can save 1.5~40× energy consumption and 9~873× computing latency under the same bit-width configuration.

II. BACKGROUND

A. DNNs and AiMC

From MLP to CNNs to today's popular attention neural networks, DNN models in distinct forms to implement complex perceptual functions. Despite the variety of calculation types of these models, matrix multiplication calculations have always been their main requirement. Fig. 2(a) shows the typical prototype of attention computing in transformer[5], and the equation is:

$$\text{Attention}(Q, K, V) = \text{Softmax}\left(\frac{QK^T}{\sqrt{d_k}}\right)V \quad (1)$$

Where Q , K , and V are large-scale matrices with $N \times d_k$ dimension; d_k is a scaling factor related to d_{model} ; N is the token number; d_{model} is an embedding size for each token, and Softmax is a nonlinear activation function. In this expression, the matrix multiplication operations caused by Q , K , and V reach more than 90% of the total computation. It also represents the situation for the other DNNs. Therefore, optimizing matrix calculations is already the main goal of current DNN accelerators. Benefiting from the robustness and quantization of neural network algorithms, recently, more researchers have started using AiMC technology for high-performance VMM. Fig. 2(b) demonstrates the brief rationale of this technology for QK^T calculation.

B. Large-Scale Multibit AiMC Challenges

The growing complexity of DNNs prompts the demand for multibit and large-scale matrix calculation for higher algorithm accuracy. This will bring serial key challenges:

Signal Margin and Computing Linearity. Fig. 3(c) shows an AiMC circuit that implements multiply-accumulate computing (MAC) based on current-mode. Each MCC (memory and computing cell) uses a pair of transistors to support 1-bit analog multiplication and the result current is pooled on the output line (OL) to realize the full-parallel analog accumulation. It suffers from small signal margin and low computational linearity due to limited voltage swing and the influence of the transistor's process variations and inherent I_{DS} characteristics (see Fig. 3(a) green and red lines).

Multibit Operations Efficiency. Multibit operations are crucial for handling complex neural network computations efficiently. However, the traditional AiMC hardware just supports small and low bit-width VMM, which require additional circuitry or cycles to extend the size and bit-width of the computation (see ❶ in Fig. 3(b)). For multibit input, existing bit serial mechanisms slow down the AiMC, and for multibit weight, each output channel requires data conversion, which greatly increases the usage count of ADCs and energy consumption. Thereby, some works start to explore weighted calculations in-analog domain. Recent works [6] and [7] proposed C-ladder and C-2C ladder scheme for multibit weighting computation, respectively (see ❷ and ❸ in Fig. 3(b)). However, they can only perform one multiplication each clock cycle, which has limited parallelism. Meanwhile, they still need DAC as input data conversion. Currently, analog computing circuits do not demonstrate a significant advantage in performing multibit operations.

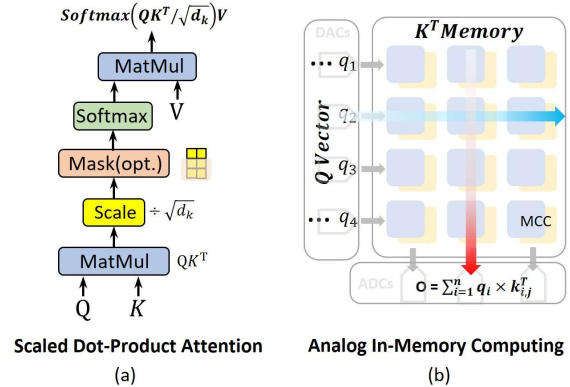


Fig. 2. (a) Scaled Dot-Product Attention. (b) AiMC topology.

Data Movement Cost. As the scale of computation increases, the cost of long-distance and high-frequency inputs and partial sums (weight keeps silence in memory) in registers becomes more significant in current AiMC accelerators (see Fig. 3 (c)). Taking an example in PRIME[3], more than 80% of energy and latency are caused by data movement. To this end, some technical recommendations alleviate this dilemma by enhancing data locality and reuse. For example, [8] combines systolic array within DiMC architecture to realize the shortest distance data movement between regularly arranged DiMC macros, and [4] utilizes a current mirror to achieve direct connection along the column of AiMC macros. However, these solutions still face the problem of high peripheral circuit overhead.

DACs/ADCs Overhead. In the AiMC system, DACs and ADCs have always been the primary consumers of energy and area (see Fig. 3(d)) (70% at least[9]). A series of proposals has been proposed to alleviate this dilemma. In DAC circuits, the bit-serial input scheme has been suggested to reduce the overhead of input. However, it comes at the cost of increasing ADCs. In ADC circuits, although there are some novel ADC solutions, such as time-based, CCO-based, and counter-based ADC, none of them can solve the current problem.

C. In-Charge Compute and In-Time Connect Opportunities

To overcome these challenges and unlock the full potential AiMC, we focus mostly on in-charge computing and in-time interconnect.

Opportunities #1: Compared with current-mode computing, in-charge computing is implemented through charge sharing between switching capacitors, which has the advantage of higher precision. Fig. 3(e) shows a popular MCC and array structure for implementing charge-domain AiMC operations. Performing calculations in capacitors not only has a higher resistance to PVT (processing, voltage, and temperature) variations, but also avoids the influence of the nonlinear area of the transistor, which makes the calculation more linear (see Fig. 3(g) green line). As discussed earlier, this calculation method still faces the problem of multi-bit calculation efficiency because each switch capacitor only supports 1-bit MAC. Fortunately, inspired by the proportional presence of switched capacitors in ADC/DACs and prior work[10], we can group the capacitances originally present in the array to create a weighted effect. We will discuss this method in section III.

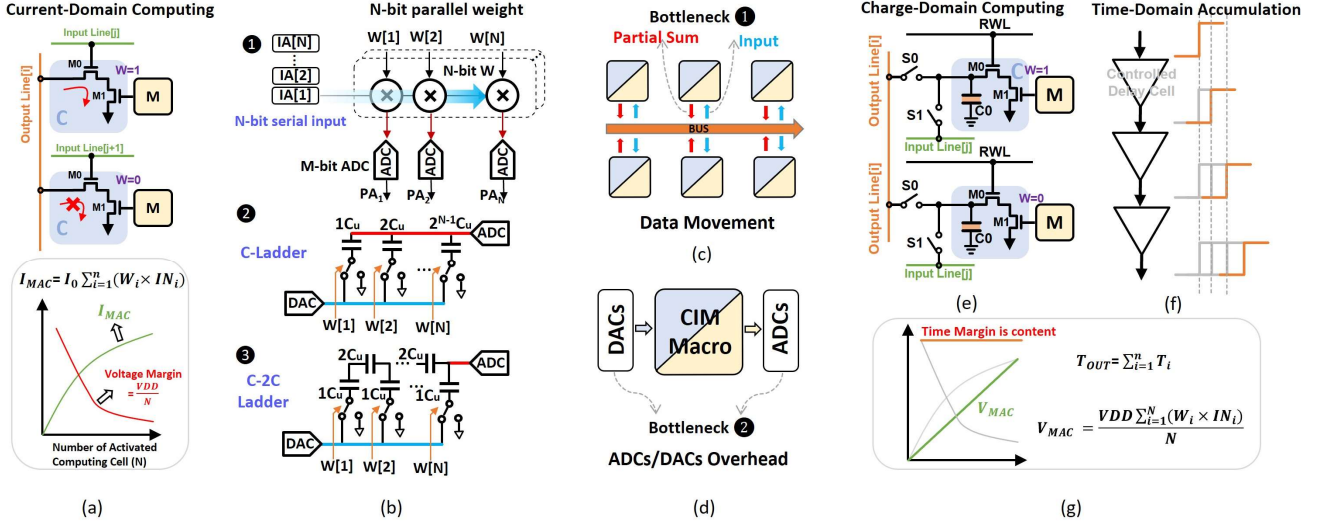


Fig. 3. Multibit and large-scale AiMC Challenges: (a) limited signal margin and low linearity of current-domain computing; (b) low-efficiency multibit computing; (c) the bottleneck of data movement; (d) the over cost of AD/DA conversion, and Opportunities: (e) high linear in charge-domain computing and (f) high signal margin in time-domain accumulation.

Opportunities #2: Regardless of the calculation operation in current-domain or charge-domain, the result is in the form of voltage, which causes signal margin issues due to limited supply voltage range. This limits the parallelism of analog calculations. Therefore, we can consider ways to interconnect analog voltage signals in time-domain to further increase the scale of AiMC without margin problem. Fig. 3(f) shows the principle of time-domain interconnecting and the relationship between signal margin and computing parallelism.

III. AiDAC ARCHITECTURE

A. Overview

The overall AiDAC architecture is shown in Fig. 4(a), which comprises input and output buffer, row drivers (see ① in Fig. 4(b)), column time accumulators (see ② in Fig. 4(b)), charge-domain (C-D) macros, time-domain ADCs (TDCs), and controller. In AiDAC architecture, multibit digital input signals are broadcasted through row drivers to horizontal C-D macros and in-situ computing is carried out with the pre-stored multibit weights to get MAC voltages; after that, the column time accumulators transform and summarize voltage results into MAC time signal along the vertical macros; finally, the time signals are converted into digital MAC output by TDCs, and then written to the output buffers. Next, we will discuss our AiDAC architecture in detail.

B. Multibit In-Charge Computing

In section II-C, we discuss the characteristics of the traditional charge-domain computing paradigm, in which each MCC is equipped with a capacitor for 1-bit weighted MAC computing. In this subsection, we propose an innovative in-charge computing mechanism that directly performs high-precision input conversion and multi-bit MAC in the charge domain by grouping row and

column capacitances, which originally existed. It is worth noting that this grouping method does not require any modification of the MCC (see ③ in Fig. 4(b)).

(1) **DAC-Less Conversion by Grouping Row Capacitors.** In our design C-D macro (see ④ in Fig. 4(c)), MCCs are arranged like a crossbar, in which MCCs in the same row were divided into N groups with the ratio of $1:2:\dots:2^{N-1}$ (see blue dotted box in Fig. 4(c)). All MCCs from the same group share one input line (IL), and the ILs between adjacent groups are controlled and connected through switch S_2 . The IL in each group is connected to the output of a tri-state gate, and the input of tri-state gate is driven by the input buffer and controlled by EN terminal. When S_2 is turned off and EN is turned on, the capacitors inside the MCCs of different groups are charged or discharged according to the input binary number IN_i . Afterwards, the tri-state gate is closed and S_2 is turned on. At this time, all capacitors in the same row will take place charge sharing and get equal voltage. The relationship between conversion voltage and the digital input is:

$$V_{IN}^i = \frac{IN_i}{2^N - 1} V_{DD} \quad (2)$$

Where i the row index; V_{DD} is power voltage; and N is input bit-width. Obviously, in this mechanism, row capacitors naturally act as DAC, and each row of array just requires additional N tri-state gates and switches with negligible area and power consumption.

(2) **Single-bit Weight MAC by Column Charge Sharing.** In an MCC, analog multiplication is performed by two transistors, whose gate is controlled by RL and memory cell, respectively. When RL pulls up, each MCC separately determines whether to release the charge in the capacitor based on the 1-bit data stored in MC (“1” is kept and “0” is released). The charge present in the capacitor represents the result of multiplying between N -bit input and 1-bit weight. After the multiplication is completed, the S_0 switch is turned on, and the capacitors in the MCCs in the same column share charges to true the full parallel accumulation

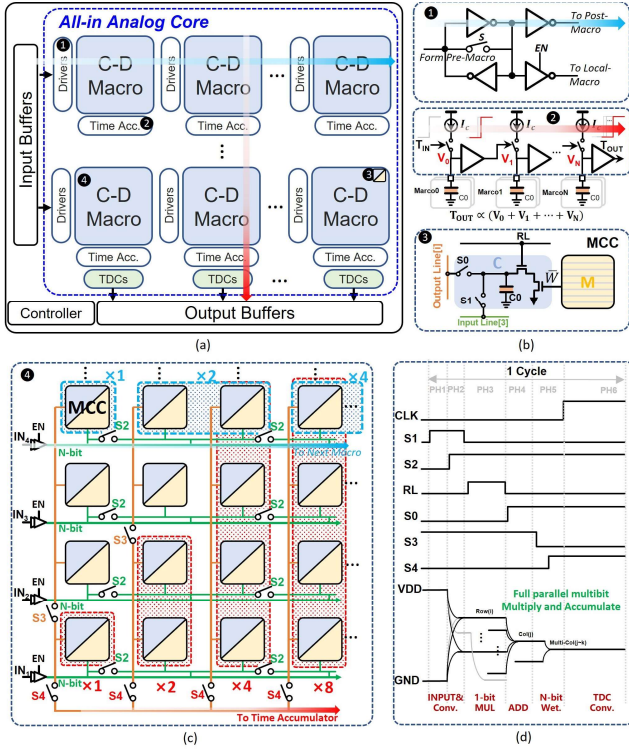


Fig. 4. An illustration of the (a) AiDAC architecture; (b) row driver, column time accumulator, MCC; (c) MCC array; and (d) the operation time diagram of AiDAC.

process. Then the output voltage after charge sharing in the j^{th} column can be expressed as:

$$V_{out}^j = \sum_{i=1}^M \frac{V_{IN}^i \times W_{i,j}}{M} \quad (3)$$

Where M is the total number of rows of a C-D macro; $W_{i,j}$ is the 1-bit weight of the i^{th} row and j^{th} column.

(3) In-situ Weighted Expansion by Grouping Column-to-Column Capacitors. We can implement multibit weighted computing by configuring the number of column-to-column capacitors involved in charge sharing. In N -bit MAC with M input channels, N columns are organized as a compute block (CB); all MCCs in the first column are divided into two groups with the ratio of 1 to $M-1$ through switch $S3$; the second column is 2 to $M-2$; by analogy, the N^{th} column is 2^{N-1} to $M-2^{N-1}$. Thereby, the ratio of the number of MCCs listed to output between N columns in a CB is 1: 2: \dots : 2^{N-1} (see the red dotted box in Fig. 4(c)). When a CB computing finished, $S3$ is turned off, and then $S4$ is turned on, and we can get the expression of output voltage of a CB:

$$V_{OUT} = \frac{\sum_{j=1}^N 2^j \times V_{out}^j}{2^N - 1} \quad (4)$$

Where j is the column index in a CB; N is the weight bit width; and V_{out}^j is the output voltage of j^{th} column.

C. Large-Scale Interconnect in Analog-Domain

Usually, multiple AiMC macros need to be interconnected to meet the computing needs of large-scale DNN algorithms. Compared with traditional analog calculation to digital conversion to digital interconnection (AC-DC-DI) pathway, the method of directly interconnecting these analog results in the analog domain (AC-AI) not only reduces the distance of data movement and improves the degree of data reuse, but also decreases the conversion times, which has advantages in energy-efficiency. In this subsection, we offer a new all-analog large interconnection mechanism.

(1) Gate Control Row Driver. Thanks to the precious CD macro design proposed in the previous subsection, the input can be driven directly into the MCCs without DACs. Therefore, we use row drivers as horizontal bridges between macros. As shown in Fig. 4(b), it consists of four inverters. The first two inverters are connected in the form of a latch with high response speed. The next two inverters can invert the signal and keep the output having a similar shape to the input from previous macro, and among them, the output of top inverter is propagated to the next macro, and the output of bottom inverter is used in the local macro. The bottom inverter can be power gating by EN terminal to save energy. Switch S will turn on during reset phase.

(2) Column Time Accumulator. In our design, each CB of each C-D macro generates a voltage, which represents a partial sum. Thus, we would like exploiting column time accumulators to bridge the macros, vertically. A column time accumulator (see 2 in Fig. 4(b)) consists of serial head-to-tail voltage-to-time converters (VTCs)[11]. Whenever the previous VTC completes a signal transition, it will release a pulse signal to drive the post VTC to work. The start pulse signal is input from the top VTC, and the stop pulse signal is collected from the bottom VTC. In this schedule, the voltage signal is converted into time signal for accumulation. Finally, TDC can convert the time difference between the start and stop signal as a complete digital summation output. Considering the inherent delay in the circuit, we use a redundant column, which can be shared to the entire macro, as a reference, and the output of this reference column is input into the TDC as the actual start signal.

D. Full Parallel Inference

The AiDAC architecture can perform fully parallel computation in one clock cycle. Fig. 4(d) shows the timing diagram of AiDAC in six phases: **Phase I** (Input): $S1$ "ON", EN enable, and $S2$ turn off; row capacitors are charged or discharged according to binary input. **Phase II** (Input Conversion): $S2$ "ON"; row capacitors to share charging and in progress digital to voltage conversion. **Phase III** ($N \times 1$ -bit Multiply): $S1$ "OFF" and RL set high; multi-bit input voltages and local 1-bit weight perform in-situ multiplication. **Phase IV** (Full-Parallel Add): RL set low and $S0$ turn on; charge share in the same column capacitors and execute full-parallel accumulation. **Phase V** (N -bit $\times N$ -bit Multiply): Switch $S3$ turn on, wait a moment, switch $S4$ "ON"; capacitances between columns share charge and perform multi-bit weighting calculations. **Phase VI** (Output Conversion): Switch $S3$ and $S4$ hold, TDCs and time accumulators enable; The result voltages between vertical macros are accumulated in the form of time and converted into digital signal by TDC.

IV. EVALUATION

A. Experiment Setup

AiDAC Configuration. The AiDAC architecture is configured in three levels. At the cell level, each MCC adopts a 2-fF MOM capacitor for arithmetic and a cluster with 8 6T-SRAMs as example storage. The MOM capacitor is stacked above the storage cluster without additional area cost. At the macro level, we set each macro includes 128×256 MCCs, 128 row drivers, and 32 column time accumulators. Each CB has 8 columns MCCs, and each CB has a time accumulator. At the core level, each core consists of 64 macros, 256 TDCs, 2KB input buffers, and 2KB output buffers. For AiDAC's specific components, we adopt silicon-verified results for TDCs[12] and use simulated results by Cadence for row drivers, column time accumulators, and charge domain computing circuit. We also use data from CACTI[13] to evaluate the latency, area, and energy of input and output buffer. The energy and area consumption of auxiliary digital parts, such as row and column decoders, etc. are small enough compared to the above analog portion so it is neglected here. Simulations are under an industry standard 28nm CMOS process with 0.9V power supply, 50MHz clock rate for analog part and 1GHz for digital part. The detailed parameters are shown in Table I.

Table I. Summary of AiDAC Parameters and Performance

	Compo.	Num. & Size	Energy (pJ)	Area (μm^2)	Latency (ns)
Cell	Capacitor	2fF	-	0.8	-
	6T SRAM	8	-	0.095	-
Macro	MCC	128×256	0.81fJ/act.	0.8	-
	Row driver	128	9.36fJ	0.18	<30ps
	Time Acc.	32	58.5fJ	5.3	113ps
Core	Macro	8×8	^a 29.6	262193	13ns
	^b TDC (8bits)	32×8	7.7	6865	0.9
	I/O buffer	4KB	2.9/256b	4656	0.112/256b
Total	2MB SRAM		4235	18.5mm^2	<20/VMM

^a50% MCC activate; ^b Silicon-Verified by [12]

Benchmark. To show the effectiveness of multibit computing precision of our AiDAC, the evaluation is performed using 4 complex DNNs, which includes 4 CNNs model (CNN-3, AlexNet VGG-8, Resnet-18) and 1 large language model (BERT) which is transformer based. All 5 benchmarks are quantized into 8-bit.

B. Experiment Results

Precision. Fig. 5(a) illustrates the transfer curve (TC) between input binary code and conversion voltage. The corresponding integral nonlinearity (INL) and differential nonlinearity (DNL) are shown in Fig. 5(b). Overall, their output errors are all less than two least significant bits (LSB), but in most cases, the errors are less than one LSB. We also evaluate the circuit error under the influence of PVT. As shown 2K Mento-Calo simulation in Fig. 5(c), the 3σ variation of input conversion is 2.25mV at room temperature, TT corner, and 0.9V power supply, which is less than voltage of 1 LSB (3.52mV). Fig. 5(d) shows two TCs during in-charge 8-bit MAC with 128 channels. Among them, the blue curve represents the MAC voltage transformation when stored weights scan from 0 to 255 and input stays at 255. The red curve

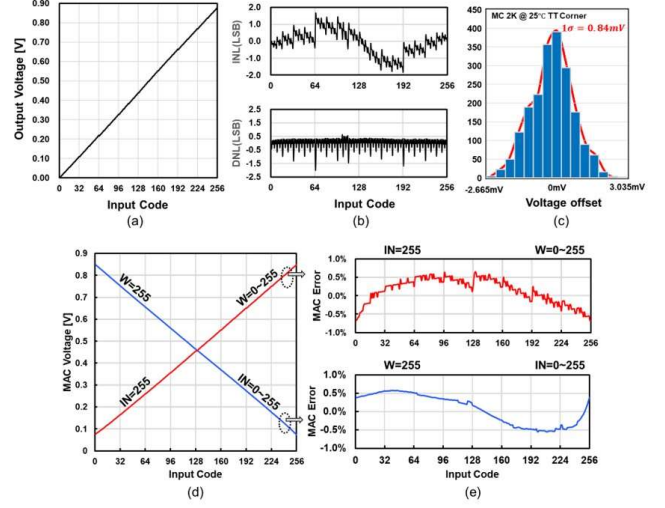


Fig. 5. An illustration of the (a) Transfer curve (TC) between input code and output voltage; (b) INL and DNL of TC; (c) input conversion error under 2K Mento-Calo simulation; (d) two TCs during 8-bit MAC with 128 input channels; and (e) correspond MAC error.

is got by scanning input (0~255) and keeping weight (255). We also can extract the MAC error curves in the above TCs (see Fig. 5(e)). The result shows the maximum MAC error does not exceed 0.68%. The time accumulator is designed with reference[11], and its error is less than 0.11%. It's clear claim that our proposed charge domain method has excellent linear performance and accuracy for multibit computing. Through the above simulations we observe less than 0.5% inference accuracy loss across all 5 benchmarks. It's clear that our AiDAC has excellent accuracy for multibit computing for AI applications.

Energy Efficiency and Throughput are evaluated with 8bits weight and 8bits activation. According to the summary in Table. I, when executing a full-parallel 8-bit VMM with 1024×256 scale, entire core about consumption 4.235nJ energy and 20ns latency under 50% calculation sparsity (sparsity configuration is based on the average output of the neural network [14]). An AiDAC core can reach up to 123.8TOPS/W in energy efficiency according to the formula "energy-efficiency = $(1024 \times 256 \times 2) / (4.235\text{nJ})$ " and can reach up to 26.2TOPS in throughput according to the formula "throughput = $(1024 \times 256 \times 2) / (20\text{ns})$ ", which multiplication and addition both count as one operation. We compare our AiDAC with 8 SOTA IMC architectures[7, 9, 15-20], which have different technical primitives. As shown in Fig. 6, AiDAC, on average, improves energy efficiency by 1.5~40 times and enhances throughput by 9~873 times.

C. Analysis and Discuss

The performance of the AiDAC architecture is mainly benefiting from the effectiveness of innovative all-analog computation and interconnection methods. It can be summarized into three key points: First, in-charge computing ensures the matrix operation accuracy. Compared to other advanced AiMC circuits, AiDAC further reduces VMM error to 0.79% (see Fig. 7(a)). Second, charge-share mechanism drives multibit data generation and

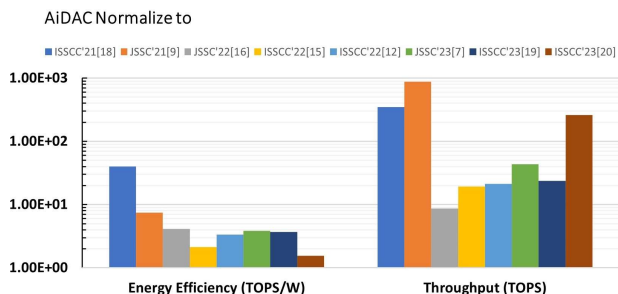


Fig. 7 The normalized VMM (a) energy efficiency and (b) throughput of AiDAC over other SOTA IMCs design.

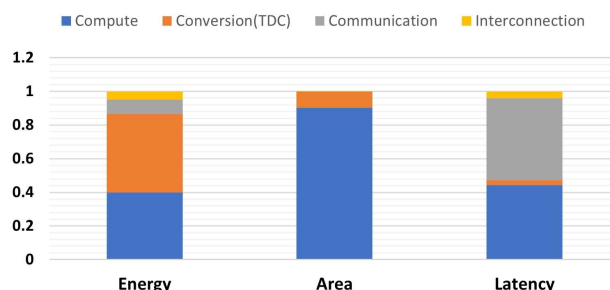


Fig. 8. Overhead of different operations in AiDAC.

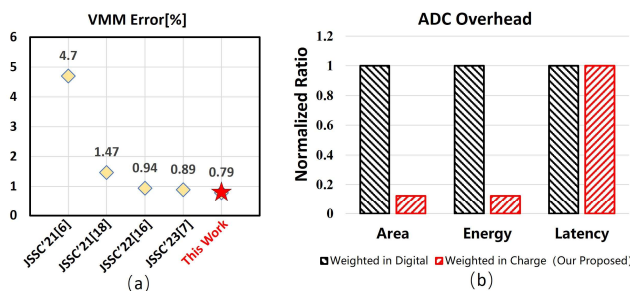


Fig. 6. (a) VMM error and (b) ADCs overhead comparison.

operation all in analog, which avoids the demand for DACs and exponentially reduces the number of times ADC is used. Compared to weighted in digital, the energy and area consumption of ADCs can be reduced by 87.5% (see Fig. 7(b)). Finally, local analog inter-connect is another way to improve performance. Data movement locally helps diminish the energy and latency of data routing. Analog connection contributes to drop interface circuit waste, each ADCs/DACs can be shared by more macros. Fig. 8 shows the percentage overhead of interconnection, conversion, compute, and communication in AiDAC.

V. CONCLUSION

In this paper, we propose AiDAC architecture for accelerating high-performance VMM. All computing processes are executed in analog domain, which improve multibit operations and data movement efficiency. Our AiDAC shows excellent performance in energy efficiency (123.8TOPS/W), throughput (26.2TOPS), and precision (<0.79% VMM error) and first indicates the excellent advantage of AiMC in multibit computing. In the future, this technology can also be generalized to other IMC architectures with different memory types.

ACKNOWLEDGMENTS

This work was supported in part by the National Key Research and Development Program of China under Grant 2019YFB2204800 and in part by the Strategic Priority Research Program of Chinese Academy of Sciences, under Grant XDB44000000.

REFERENCE

- [1] Y. Chen *et al.*, "A survey of accelerator architectures for deep neural networks," *Engineering*, vol. 6, no. 3, pp. 264-274, 2020.
- [2] S. Yu *et al.*, "Compute-in-Memory Chips for Deep Learning: Recent Trends and Prospects," *IEEE Circuits and Systems Magazine*, vol. 21, no. 3, pp. 31-56, 2021.
- [3] P. Chi *et al.*, "PRIME: a novel processing-in-memory architecture for neural network computation in ReRAM-based main memory," in Proceedings of the 43rd International Symposium on Computer Architecture, Seoul, Republic of Korea, 2016, pp. 27-39.
- [4] W. Li *et al.*, "TIMELY: pushing data movements and interfaces in PIM accelerators towards local and in time domain." pp. 832-845.
- [5] A. Vaswani *et al.*, "Attention is all you need," *Advances in neural information processing systems*, vol. 30, 2017.
- [6] S. Xie *et al.*, "16.2 eDRAM-CIM: Compute-In-Memory Design with Reconfigurable Embedded-Dynamic-Memory Array Realizing Adaptive Data Converters and Charge-Domain Computing." pp. 248-250.
- [7] H. Wang *et al.*, "A Charge Domain SRAM Compute-in-Memory Macro With C-2C Ladder-Based 8-Bit MAC Unit in 22-nm FinFET Process for Edge Inference," *IEEE Journal of Solid-State Circuits*, pp. 1-14, 2023.
- [8] X. Chen *et al.*, "A Systolic Computing-in-Memory Array based Accelerator with Predictive Early Activation for Spatiotemporal Convolutions." pp. 1-5.
- [9] X. Si *et al.*, "A Local Computing Cell and 6T SRAM-Based Computing-in-Memory Macro With 8-b MAC Operation for Edge AI Chips," *IEEE Journal of Solid-State Circuits*, vol. 56, no. 9, pp. 2817-2831, 2021.
- [10] J. Kim *et al.*, "A Charge Domain P-8T SRAM Compute-In-Memory with Low-Cost DAC/ADC Operation for 4-bit Input Processing."
- [11] P. Chen *et al.*, "A 31- μ W, 148-fs Step, 9-bit Capacitor-DAC-Based Constant-Slope Digital-to-Time Converter in 28-nm CMOS," *IEEE Journal of Solid-State Circuits*, vol. 54, no. 11, pp. 3075-3085, 2019.
- [12] Q. Chen *et al.*, "A Single-Channel Voltage-Scalable 8-GS/s 8-b >37.5-dB SNDR Time-Domain ADC With Asynchronous Pipeline Successive Approximation in 28-nm CMOS," *IEEE Journal of Solid-State Circuits*, vol. 58, no. 6, pp. 1610-1622, 2023.
- [13] N. Muralimanohar *et al.*, "CACTI 6.0: A Tool to Understand Large Caches."
- [14] Z. Xuan *et al.*, "High-Efficiency Data Conversion Interface for Reconfigurable Function-in-Memory Computing," *IEEE Transactions on Very Large Scale Integration (VLSI) Systems*, pp. 1-14, 2022.
- [15] F. Tu *et al.*, "A 28nm 29.2TFLOPS/W BF16 and 36.5TOPS/W INT8 Reconfigurable Digital CIM Processor with Unified FP/INT Pipeline and Bitwise In-Memory Booth Multiplication for Cloud Deep Learning Acceleration." pp. 1-3.
- [16] H. Jia *et al.*, "Scalable and Programmable Neural Network Inference Accelerator Based on In-Memory Computing," *IEEE Journal of Solid-State Circuits*, vol. 57, no. 1, pp. 198-211, 2022.
- [17] P. C. Wu *et al.*, "A 28nm 1Mb Time-Domain Computing-in-Memory 6T-SRAM Macro with a 6.6ns Latency, 1241GOPS and 37.01TOPS/W for 8b-MAC Operations for Edge-AI Devices." pp. 1-3.
- [18] Z. Chen *et al.*, "CAP-RAM: A Charge-Domain In-Memory Computing 6T-SRAM for Accurate and Precision-Programmable CNN Inference," *IEEE Journal of Solid-State Circuits*, vol. 56, no. 6, pp. 1924-1935, 2021.
- [19] B. Wang *et al.*, "A 28nm Horizontal-Weight-Shift and Vertical-feature-Shift-Based Separate-WL 6T-SRAM Computation-in-Memory Unit-Macro for Edge Depthwise Neural-Networks." pp. 134-136.
- [20] S. E. Hsieh *et al.*, "7.6 A 70.85-86.27TOPS/W PVT-Insensitive 8b Word-Wise ACIM with Post-Processing Relaxation." pp. 136-138.